Clinica Chimica Acta xxx (2011) xxx–xxx

Contents lists available at ScienceDirect

Clinica Chimica Acta

journal homepage: www.elsevier.com/locate/clinchim

High-resolution melting curve (HRM) analysis to establish *CYP21A2* mutations converted from the *CYP21A1P* in congenital adrenal hyperplasia

Yi-Ching Lin [a,b], Yu-Chih Lin [c], Ta-Chi Liu [a,b,d], Jan-Gowth Chang [a,b,e,f,*], Hsien-Hsiung Lee [g,**]

[a] Institute of Clinical Medicine, Kaohsiung Medical University, Kaohsiung 807, Taiwan
[b] Department of Laboratory Medicine, Kaohsiung Medical University Hospital, Kaohsiung Medical University, Kaohsiung 807, Taiwan
[c] Division of General Internal Medicine, Department of Internal Medicine, Kaohsiung Medical University Hospital, Kaohsiung Medical University, Kaohsiung 807, Taiwan
[d] Division of Hematology and Oncology, Department of Interal Medicine, Kaohsioung Medical University Hospital, Kaohsioung Medical University, Kaohsioung, Taiwan
[e] Center for Excellence in Environmental Medicine, Kaohsiung Medical University, Kaohsiung 807, Taiwan
[f] Cancer Center, Kaohsiung Medical University Hospital, Kaohsiung 807, Taiwan
[g] School of Chinese Medicine, College of Chinese Medicine, China Medical University, 91 Hsueh-Shih Road, Taichung 404, Taiwan

ARTICLE INFO

Article history:
Received 2 June 2011
Accepted 24 June 2011
Available online xxxx

Keywords:
CYP21A2
CAH
HRM
PCR-based amplification
Mutational detection
Heteroduplex
Homoduplex

ABSTRACT

Background: Congenital adrenal hyperplasia (CAH) is an autosomal recessive disease of an inborn error of steroid metabolism in humans. More than 90% of CAH cases are caused by mutations of the steroid 21-hydroxylase (*CYP21A2*) gene, and approximately 75% of the defective *CYP21A2* genes are generated through an intergenic recombination with the neighboring *CYP21A1P* pseudogene.
Methods: A high-resolution melting (HRM) curve analysis was designed to characterize 11 mutation sites of the *CYP21A2* gene that commonly appeared in 21-hydroxylase deficiency. Among these 11 mutations, 9 were found in CAH patients, and 2 were mutations created from normal individuals.
Results: From the HRM analysis using 6 fragments of amplicons, we have successfully identified these 11 common disease-causing mutations of the *CYP21A2* gene, among which 3 showed 3 distinguishable melting plots; the heteroduplexes showed an upcurved plot, a horizontal plot of homoduplexes of wild-type (WT), and a downcurved plot of homoduplexes of compound mutations.
Conclusions: The HRM analysis is a 1-step of non-gel resolution technique which saves time and is a low-cost method to undertake such a program for screening CAH patients with the 21-hydroxylase deficiency caused by intergenic conversions from the neighboring *CYP21A1P* pseudogene.

1. Introduction

Congenital adrenal hyperplasia (CAH) is an autosomal recessive disease of an inborn error of steroid metabolism in humans. It may produce excessive or deficient sex steroids and can alter development of primary and secondary sex characteristics. There are 6 enzymes, cholesterol side-chain cleavage enzyme (*CYP11A*), *CYP17* (17, 20-lyase), steroid 21-hydroxylase (*CYP21A2*), steroid 11-beta-hydroxylase (*CYP11B1*), steroid 18-hydroxylase (*CYP11B2*), and 17β-hydroxylsteroid dehydrogenase, that are required for the synthesis of steroid hormones. However, more than 90%–95% of all CAH cases are caused by a *CYP21A2* deficiency [1]. There are 3 forms of CAH: the classical salt-wasting, classical simple virilizing, and non-classical forms [2,3]. The incidence of the classical form of CAH disease is reported to be 1:10,000–1:18,000, depending on race [1,4] while the non-classical form is milder and commonly occurs in the general population at a rate of 1:1700 [3,5].

The gene coding for P450c21 is designated *CYP21A2*. A duplicate copy designated *CYP21A1P* exists which shares 98% nucleotide sequence homology with *CYP21A2* in exons and 96% in non-coding sequences [6,7]. These two genes are separated by 30 kb in chromosome 6p21.3 adjacent to and alternating with the *C4A* and *C4B* genes encoding the fourth component of the serum complement and show great similarity. This seems the most likely reason for misalignment and gene conversions to occur during meiosis [8]. Under this circumstance, genetic defects of the *CYP21A2* gene in CAH may commonly lead to 1 of 2 categories of (a) small-scale conversions of the *CYP21A1P* sequence (commonly 1 of 11 mutations) [9] and (b) chimeras of the chimeric *CYP21A1P*/*CYP21A2* and *TNXA*/*TNXB* genes [10–12]. The *CYP21A1P* is a nonfunctional gene which was thought to carry 15 mutations [6,7]. However, a study of ethnic Chinese (i.e., Taiwanese) [13] indicated that not every healthy individual ($n = 100$) bears these mutations, which had an approximately 90% in the population frequency [13], and 4 loci of the I2 splice (including nt 707–714del), I172N, cluster E6, and F306ΛL307insT were processed by "complete" selective pressure in evolution [13]. The *CYP21A2*

* Correspondence to: J.-G. Chang, Department of Laboratory Medicine, Kaohsiung Medical University Hospital, 100 Shih-Chuan 1st Rd., Kaohsiung 870, Taiwan. Tel.: +886 7 3115104; fax: +886 7 3213931.
** Correspondence to: H.-H. Lee, School of Chinese Medicine, College of Chinese Medicine, China Medical University, 91 Hsueh-Shih Road, Taichung 404, Taiwan. Tel./fax: +886 3 9389073.
E-mail addresses: jgchang@ms.kmuh.org.tw (J.-G. Chang), hhlee@mail.cmu.edu.tw,

0009-8981/$ – see front matter © 2011 Published by Elsevier B.V.
doi:10.1016/j.cca.2011.06.033

Please cite this article as: Lin Y-C, et al, High-resolution melting curve (HRM) analysis to establish CYP21A2 mutations converted from the CYP21A1P in congenital adrenal hyperplasia, Clin Chim Acta (2011), doi:10.1016/j.cca.2011.06.033

deficiency in our population (i. e., Taiwanese), approximately 81% of which are defective *CYP21A2* genes [14], is generated through an intergenic recombination [9] with the neighboring *CYP21A1P* pseudogene. Among them, the 3 most common mutations of the *CYP21A2* gene in ethnic Chinese (i.e., Taiwanese) of 69% frequencies are the I2 splice (nt 655, IV2-12A/C>G) (34%, $n=400$ chromosomes), I172N (23.5%), and R356W (11.8%) [14], which show high similar incidences worldwide in different races [1,15,16]. The frequency of other mutations such as Q318X, F306-L307insT, and cluster E6 are about 12% [14]. A mutation of V281L, the most common nonclassical disease appearing in high frequency in patients in France, Austria, Italy, Spain, Turkey, Argentine, and Portugal [15–17], was not found in Taiwanese [18], Japanese [19], or Tunisian patients [20].

Polymerase chain reaction (PCR) amplification is an indispensable tool for detecting a gene of interest in current molecular biology. The molecular diagnosis of the *CYP21A2* deficiency through direct analysis of the *CYP21A2* gene was proven to be feasible and accurate. To isolate the *CYP21A2* gene free from the *CYP21A1P* pseudogene, several methods including 1-step [21,22] and 2-step methods [23–25] for amplification of the *CYP21A2* gene were developed. These PCR products with either 1 or 2 fragments as a template are subject to known or unknown mutational detection using more-practical methods, such as PCR/ligase detection [24], single-stranded conformation polymorphism (SSCP) [26], amplification-created restriction site (ACRS) [27], real-time PCR [28], denaturing high-performance liquid chromatography (DHPLC) [18], multiplex minisequencing [29], laser desorption/ionization time-of-flight (MALDI-TOF) [30], and multiple ligation-dependent amplification (MLPA) assay to detect the *CYP21A2* gene [31].

The aim of the present study was to use a high-resolution melting curve (HRM) analysis to directly identify 11 nucleotide sequences commonly appearing in the *CYP21A1P* gene, including p.P30L, the I2 splice, nt 707–714del, p.I172N, cluster E6, p.V281L, F306ΔL307inseT, p.Q318X, and p.R356W and to establish such a rapid and precise screening tool for CAH patients which account for 70%–80% of CAH cases.

2. Materials and methods

2.1. DNA samples

Genomic DNA was collected from 200 CAH patients in hospitals across Taiwan from 1994 to 2006 [14]. All families requested an extensive molecular diagnosis and provided informed consent. Among these CAH patients, 9 mutations were from the unrelated patients which accounted for about 81% of CAH cases [14] including the I2 splice where G is substituted for A/C (designated B1), deletion of 8 base pairs (bps) in exon 3 (nt707–714del, designated B2), isoleucine (ATC) at codon 172 substituted by asparagine (AAC) (p.I172N, designated C), cluster E6 (designated D), p.F306ΔL307insT (designated H2), glutamine (CAG) at codon 318 substituted by a stop codon (TAG) (p.Q318X, designated J1), and arginine (CGG) at codon 356 substituted by tryptophan (TGG) (p.R356W, designated J2) (Fig. 1). The *CYP21A2* mutations in these patients were formerly determined by the ACRS method as previously described [27]. In order to produce the heteroduplex DNA fragment for the HRM analysis, patients with the haplotype of compound heterozygous mutations in the *CYP21A2* allele were selected. Because of no patient with the p.P30L (CCG>CTG) (designated A) or p.V281L (GTG>TTG) (designated H1) mutations (Fig. 1) were found in our population [18], we created these 2 mutations from a normal individual as described previously [18].

2.2. A primary 3.5-kb differential PCR product of the CYP21A2 gene for identifying 9 mutations converted from the CYP21A1P gene

To isolate the *CYP21A2* free from the *CYP21A1P* genes, a 3.5-kb PCR product covering 10 exons of the *CYP21A2* gene was amplified with a differential paired primer, BF1/21BR (Fig. 1), as described previously [21]. To identify the *CYP21A2* mutations converted from the *CYP21A1P* gene, the 3.5-kb primary PCR products obtained from these CAH samples were then used as templates to detect the 9 mutation sites.

2.3. A primary 3.0-kb PCR product containing a mixture of the CYP21A2 and CYP21A1P genes for creating P30L and V281L heterozygous mutations in a normal individual

Because of no patient with the p.P30L or p.V281L mutations was found in our population [18], a 3.0-kb PCR product was amplified with a universal paired primer, CYP-270f/Ex10R [18] (Fig. 1), to create the p.P30L and p.V281L heterozygous mutations in 1 normal individual as previously described [18]. The 3.0-kb PCR product contained a mixture of the *CYP21A2* and *CYP21A1P* genes which present the haplotype of compound heterozygous mutations with 11 defective alleles as does the *CYP21A1P* gene [6]. The 3.0-kb PCR product was then used as a template to identify mutations of p.P30L (designated A) and p.V281L (designated H1) (Fig. 1).

2.4. Secondary PCR amplification of both the 3.5-kb and 3.0-kb PCR products for the HRM analysis

The 3.5-kb PCR products amplified with the paired primer, BF1/21BR, from these selected CAH samples and the 3.0-kb PCR product amplified with the universal paired primer, CYP-270f/Ex10R, creating p.P30L and p.V281L mutations from a normal individual were used as templates for secondary PCR amplification by HRM primers. There were 6 paired primers for the HRM analysis to detect 11 mutational loci. The sequence and location of these HRM primers are listed in Table 1.

2.5. HRM analysis

The HRM analysis included a PCR reaction, DNA melting process, and gene scanning for data analysis. These 3 programs can be performed on a single instrument. The LightCycler® 480 Real-time PCR system (Roche Diagnostics, Penzberg, Germany) with 96- or 384-well closed-tube platforms is operated by the LightCycler® 480 Gene Scanning Software (Vers. 1.5) which is an integrated, high-throughput real-time PCR instrument, and these 3 programs can be completed within 1 h.

For the PCR program, the reaction mixture for 6 secondary HRM primer PCR amplifications contained a diluted primary PCR product (3.5- or 3.0-kb PCR product), 10 μl of LightCycler®480 High Resolution Melting Master (commercially supplied, which contains FastStart Taq DNA polymerase, 2× reaction buffer, dNTP, and High Resolution Melting Dye) (Roche Diagnostics), 0.25 μM of each primer, and 2.5 mM of $MgCl_2$ in a final volume of 20 μl. The High Resolution Melting Dye only strongly binds to double-stranded (ds)DNA and has nothing to bind single-stranded (ss)DNA. The PCR conditions consisted of 2 steps: a denaturation–activation step at 95 °C for 10 min, and followed by a 45-cycle program (denaturation at 95 °C for 15 s, annealing at 60 °C for 15 s, and elongation at 72 °C for 15 s with reading of the fluorescence; by a single acquisition mode).

The melting program in this study includes 3 steps: denaturalization at 95 °C for 1 min, re-naturation at 40 °C for 1 min and then melting with a continuous fluorescent reading from 60 to 90 °C at 25 acquisitions per °C. The software system can "watch" the processes of dsDNA with fluorescence to a dissociated nothing-bound ssDNA and then processes the raw melting curve data to form a different plot. The plots obtained in the real-time stage with homozygous and heterozygous samples, respectively, are significantly different. The shapes of difference plot curves of each DNA sample must be reproducible in terms of both shape and peak height.

Gene scanning of the data analysis by the Gene Scanning Software was comprised of 3 steps: normalization of the melting curves, equilibrating to 100% as the initial fluorescence and to 0% as the

Please cite this article as: Lin Y-C, et al, High-resolution melting curve (HRM) analysis to establish CYP21A2 mutations converted from the CYP21A1P in congenital adrenal hyperplasia, Clin Chim Acta (2011), doi:10.1016/j.cca.2011.06.033

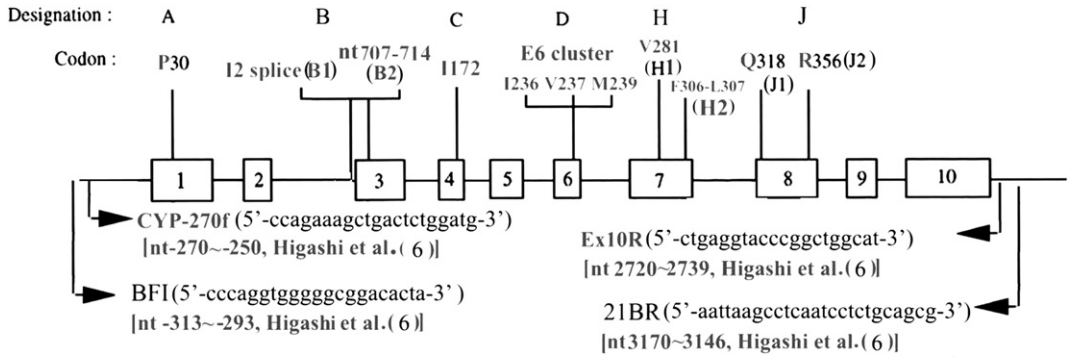

Fig. 1. Diagram of 11 *CYP21A2* mutations converted from the neighboring *CYP21A1* pseudogene and primer sequences, and locations of the amplification of the *CYP21A2* and *CYP21A1P* genes. The paired primers, BF1/21BR, were used to amplify a 3.5-kb PCR product of the *CYP21A2* gene. The universal paired primers, CYP-270f/Ex10R, were used to amplify a 3.0-kb PCR product of the mixture of the *CYP21A2* and *CYP21A1P* genes. The structure of the *CYP21A2* gene is indicated by a white box. Designations of A to J2 indicate the 11 mutation sites converted from the *CYP21A1P* pseudogene [18].

fluorescence remnant after DNA dissociation, and shifting of the temperature axis of the normalized melting curves to a point where the entire dsDNA was completely denatured. Then the difference plot analyzes differences in melting curve shapes by subtracting the curves from wild-type (WT) and mutated DNA (sequence variation), therefore differences in the plots help cluster the samples into groups.

2.6. Confirmatory sequencing for secondary HRM PCR fragments

Before the HRM analysis, the secondary PCR products amplified with the HRM paired primer (Table 1) (without using High Resolution Melting Dye) for 11 mutation sites from unrelated patients were confirmed by DNA sequencing (Supplemental Figs. 1, 2). The sequence reaction was performed in a final volume of 10 μl including 1 μl of the purified PCR product, 0.8 μl of 2.5 μM of 1 of the PCR primers, 2 μl of the ABI PRISM terminator cycle sequencing kit v3.1 (Applied Biosystems, USA), and 2 μl of 5× sequence buffer. The sequencing program was a 25-cycle PCR program (denaturation 96 °C for 10 s, annealing 50 °C for 5 s, and elongation 60 °C for 4 min), and sequence detection was performed in the ABI Prism 3130 Genetic Analyzer (Applied Biosystems).

3. Results

3.1. Use of the 3.5- and 3.0-kb PCR products for secondary HRM PCR amplification of 9 mutation sites in 9 unrelated patients and 2 created mutation sites of P30L and V281L from a normal individual

To detect the 9 mutation sites of B1, B2, C, D (cluster E6), H2, J1 and J2 (Fig. 1) from 8 unrelated CAH patients with compound heterozygous mutations (Supplemental Figs. 1, 2), a 3.5-kb primary PCR product (Supplemental Fig. 3A, lane 1) (data from only 1 patient) was generated by the paired primers, BF1/21BR. The 3.5-kb PCR product used as the template was subjected to a secondary PCR amplification (Supplemental Fig. 3B) (data from only 1 patient) using the HRM paired primers (Table 1) to produce 5 fragments of 226 bp (for loci B1 and B2 identification), 118 bp (for locus C identification), 193 bp (for cluster E6 identification), 212 bp (for locus H2 identification), and 283 bp (for loci J1 and J2 identification). On the other hand, the 3.0-kb PCR fragments (Supplemental Fig. 3A, lane 2) amplified with the paired primers, CYP-270f/Ex10R, were derived from 1 normal individual to detect 2 created mutation sites of P30L and V281L which included 2 fragments of 182 bp (for locus A identification) and 212 bp (for locus H1 identification) (Supplemental Fig. 3B) generated by the secondary amplification using the HRM paired primers (Table 1). The HRM analysis was performed on 6 different secondary PCR fragments to cover these 11 mutation sites using a 96-well plate of the LightCycler 480 system. In addition, 6 different secondary PCR products of the WT prepared from a normal individual were treated the same as those of CAH patients (data not shown).

3.2. HRM analysis of 11 different mutations in 6 different PCR fragments

Because a heterozygous DNA sample with a heteroduplex has 2 different rates of separation temperatures and while homoduplex has 1, the shapes of the melting curves obtained from these 2 samples, respectively, are significantly differed. The LightCycler® 480 Real-time PCR system has the ability to monitor this process in high resolution process to accurately document these changes. On the HRM analysis of the 182-bp amplicon (Fig. 2A) with the created heterozygous mutation of p.P30L (CCG/CTG) from the normal individual (Sc) (Supplemental

Table 1
Primers for secondary PCR amplification and the HRM analysis of the *CYP21A2* gene.

Designation	Primer (5′–>3′)	Location (nt)[a]	Amplicon (bp)	Detection locus[b]
1A2	CTGCTGGCTGGCGCCCGCCT	31–50	182	p.P30L (A)
C100	GAAGAAG GTCAGGCCCTC	602–619	226	I2 splice[c] (B1) and In3R CTTACCTCACAGAACTCCTG808–827 707–714del (B2)
E4r	AGGCACCTTGATCTTGTCTCC	808–827		
In3	TCTCCACAGCGCATGAGAGC	920–939	118	p.I172N (C)
E4r	GAGGCACCTTGATCTTGTCTCC	1016–1037		
Ex6	TCATGCTTCCTGCCGCAGTTC	1304–1324	193	Cluster E6[d](D)
C8	TGCAAAAGAACCCGCCTCATAG	1475–1496		
C9	TGCAGGAGAGCCTCGTGGCAGG	1573–1594	212	pV281L (H1) and pF306ΛL307insT (H2)
S7r	GACGCACCTCAGGGTGGTGA	1764–1785		
In7-1	In7-1 CACTCAGGCTCACTGGGTTGC	1890–1910	283	pQ318X (J1) and R356W (J2)
C12-1	ACCCTCGGGAGTCACCTGCTG	2152–2172		

[a] Based on Higashi et al. [6].
[b] Designation of A to J2 is corresponding to Fig. 1.
[c] I2 splice, IVS2 −12A/C>G or nt 655.
[d] Cluster E6 represents I236N, V236E, and M239K.

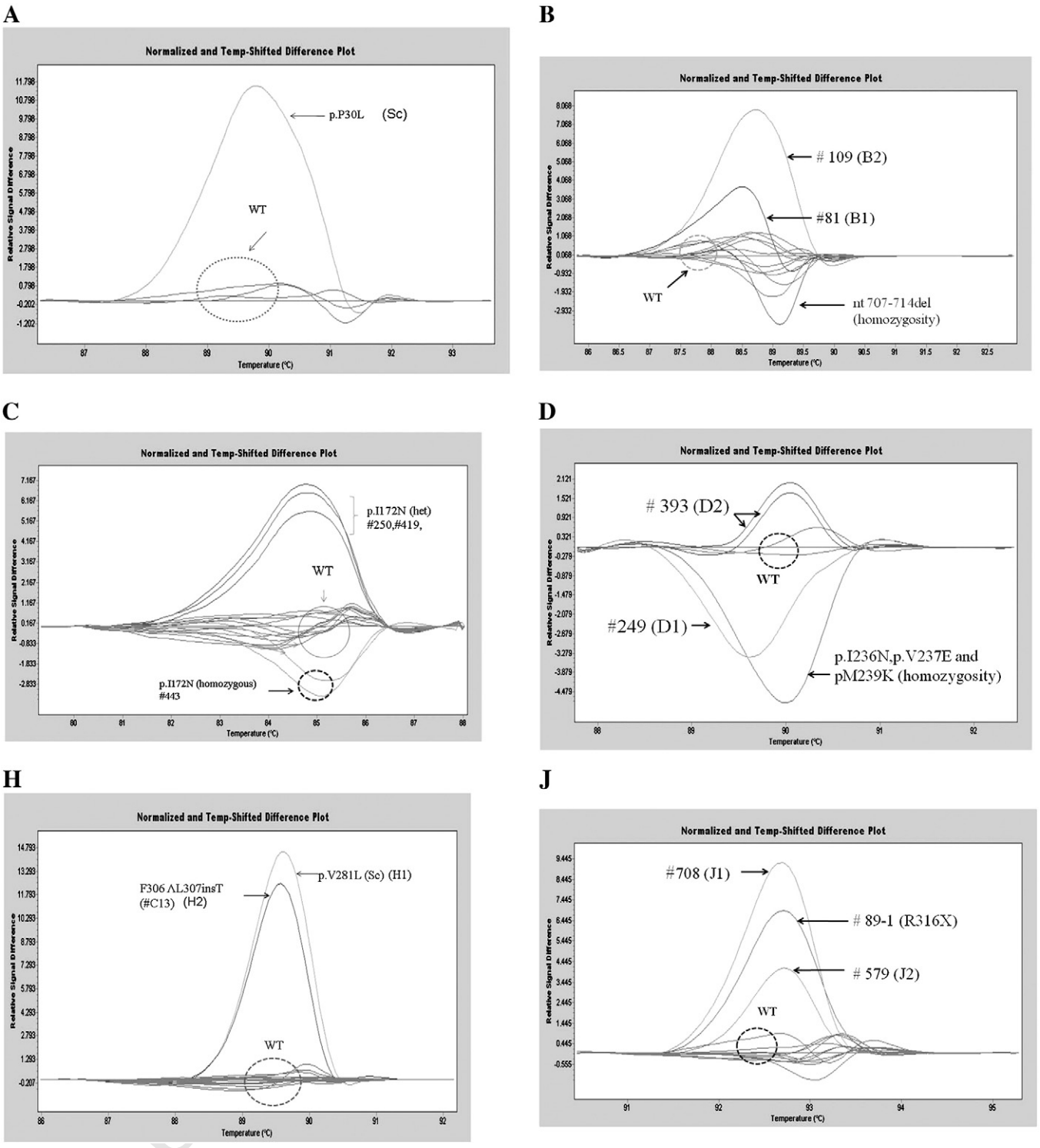

Fig. 2. Normalized and temperature-shifted difference plots of the HRM analysis for detecting 11 mutation sites of the *CYP21A2* gene from different CAH patients. Sequences A to J are designated in Fig. 1. Plot A represents a created heterozygous mutation of p.P30L in a normal individual (Sc). Plot B represents sample #81 with a heterozygous mutation of the I2 splice (B1), and sample #81 with a heterozygous mutation of 707–714del (B2). One sample with homozygous 707–714del mutations was included. Plot C represents samples #250 and #419 with a heterozygous mutation of p.I172N and sample #443 with a homozygous p.I172N mutation. Plot D represents sample #249 (D1) with a heterozygous mutation of p.I236N combined with p.V237E and sample # 393 (D2) with a heterozygous mutation of p.I236N, and pV237E combined with p.M239K. In addition, 1 sample with a homozygous mutation of p.I236N, and pV237E combined with p.M239K was included. Plot H represents a created heterozygous mutation of p.V281L in a normal individual (H1) (Sc) and sample #C13 with a heterozygous mutation of p.F306ΛL307insT (H2). Plot J represents sample #708 with a heterozygous mutation of p.Q318X, and sample #579 with a heterozygous mutation of p.R356W. One sample #89-1 with a heterozygous mutation of p.R316X was included. WT, wild-type subject; Sc, sample created; #, patient ID number.

Fig. 1A), it showed that the difference plot of the created heterozygous mutation of pP30L (CCG/CTG) (sample Sc) differentiated the one of WT subjects (CCG/CCG) (WT) ($n=3$). Obviously, unambiguous differences were present in the shapes of the melting curves for the heteroduplexes and homoduplexes. On analysis of the 226-bp amplicon with mutations of the I2 splice (IVS2-12A/C>G) (B1) and 707–714del (B2) (Fig. 2B) from 2 unrelated CAH patients (Supplemental Figs. 1B1, 1B2), sample #81 was heterozygous for the I2 splice

Please cite this article as: Lin Y-C, et al, High-resolution melting curve (HRM) analysis to establish CYP21A2 mutations converted from the CYP21A1P in congenital adrenal hyperplasia, Clin Chim Acta (2011), doi:10.1016/j.cca.2011.06.033

mutation which could easily distinguish it from WT subjects ($n=12$) and heterozygous for the 707–714del mutation of sample #109. A homozygous 707–714del was identified as a downcurved plot which differed from the horizontal plot of the WT and sample #109 with an upcurved plot. On analysis of the 118-bp amplicon with mutations of p.I172N (Table 1), the HRM analysis (Fig. 2C) showed that sample #250 (Supplemental Fig. 1C) (and sample #419) had a heterozygous mutation of p.I172N distinguished by a downcurved melting plot of the homozygous p.I172N mutation of sample #443 (sequencing data not shown) and a horizontal plot of WT subjects ($n=14$). When analyzing cluster E6 (I236, V237, and M239) (Fig. 1) of the 193-bp amplicon (Fig. 2D), there were 2 mutational types shown in Taiwanese CAH patients [14,32]. Sample #249 with heterozygous mutations of p.I236N and p.V237E (Supplemental Fig. 1D1) and sample #393 with heterozygous mutations of p.I236N, p.V237E, and p.M239K (Supplemental Fig. 1D2) showed different melting curves and were identified as different groups from WT subjects ($n=3$) by the HRM analysis. Obviously, these 2 different samples (samples #249 and #393) with 1 nucleotide difference at M239 could be distinguished. From the 212-bp amplicon for the p.V281L and p.F306ΛL307insT (Table 1) HRM analysis (Fig. 2E), the created heterozygous mutation of p.V281L of sample Sc (Supplemental Fig. 2H1) and heterozygous mutation of p.F306ΛL307insT of sample #C13 (Supplemental Fig. 2H2) could easily be distinguished from WT subjects ($n=21$), and different groups could be identified from each other. When analyzing p.Q318X and p.R356W in the exon 8 region (Fig. 1) of the 283-bp amplicon (Table 1), sample #708 with heterozygous mutations (Supplemental Fig. 2 J1) of p.Q318X and sample #579 with heterozygous mutations of p.Q318X (Supplemental Fig. 2 J2) presented upcurved plots which differed from the horizontal plot of WT subjects ($n=12$) as different groups from each other using the HRM analysis (Fig. 2F).

Obviously, the HRM analysis of the *CYP21A2* gene with 11 different mutations converted from the *CYP21A1P* pseudogene showed 3 distinguishable melting plots which included the heteroduplexes that showed an upcurved plot, a horizontal plot of homoduplexes of WT, and a downcurved plot of homoduplexes of compound mutations. In addition, polymorphic sites which influenced the heteroduplex form in the collected amplicon (Table 1) for identifying the *CYP21A2* gene are listed in Table 3

4. Discussion

CAH is a term that describes several inheritable disturbances in steroid hormone metabolism. Gene conversion, i.e., changing part of 1 gene to the sequence of a nearby homologous gene (often its pseudogene), is often the cause of genetic defects and the issue of small-scale conversions generating the defective *CYP21A2* gene is the most frequent of the 21-hydroxylase deficiencies in CAH. The wide range of CAH phenotypes is associated with multiple mutations known to affect 21-hydroxylase enzymatic activity. Clinically, mutations of the I2splice, 707–714del, the cluster E6 (I236N and V237E) [33], F306ΛL307insT, Q318X, and R356W produce a picture of the classic salt-wasting form in most patients and I172N produces the classic simple virilizing form in patients [34].

To date, PCR amplification provides the majority of samples for throughput mutational analyses. Methods for detecting a single nucleotide substitution for positional determination include ASO, PCR/ligase, ACRS, and MLPA while the SSCP and DHPLC analyses are used for non-positional detection; all of these except in the MLPA method require an agarose or PAGE preparation, and the result relies on a gel-staining or labeling process. Although direct DNA sequencing is considered the gold standard method for mutation analysis, it entails significant costs and labor and does not show the absolute sensitivity or specificity for detecting tuberous sclerosis (TSC) patients with somatic mosaicism in low-level mutant alleles [35,36]. The HRM analysis is a non-positional technique and a non-gel-based system in a closed-tube to detect mutations including polymorphisms and epigenetic differences in dsDNA samples existing in heteroduplexes and homoduplexes. Additional applications such as quantitative analysis of copy number variants, purity of PCR products, and clone identity determinations make HRM a versatile multipurpose analytical tool [37]. Compared to DNA sequencing, the HRM analysis offers cost-effectiveness for larger-scale gene screening such as DMD with 79 exons which cost €140 per patient, compared to a total of ~€800 using a direct sequencing analysis [37].

The HRM analysis was successfully applied to analyze more than 50 genes documented in the literature [38]. However, it has never been applied to detect mutations of the *CYP21A2* gene. The dependence of the scanning accuracy on the PCR product length was studied, and more errors were reported to occur as the length increases above 400 bp [39]. For high sensitivity, fragments of 150–250 bp are generally used. However, there was a successful case of scanning BRCA1 mutations up to a 600-bp amplicon [40]. Because large fragments may have more than 1 melting domain, this increases the chance that not all variants are detected. For this, the HRM analysis for *CYP21A2* mutations used a 217-bp PCR fragments on average (Table 1). In addition, SNP existing in the target gene might interfere with genotyping as described elsewhere [41]. We have pointed out that the most polymorphic region between the *CYP21A2* and *CYP21A1P* genes is located in intron 2 (IVS2) which shows an 11.2% (31/278) rate of sequence polymorphism [18]. From DNA sequencing (Supplemental Figs. 1, 2) and the *Taq*I analysis of the 3.5-kb PCR product (data not shown), sample #81 with the I2 splice and sample #109 with 707–714del mutations did not have a *Taq*I site [TCGA] at nt −198 [6]. This indicates that these 2 mutations independently resulted from an intergenic conversion. As described in another study [9], mutation of the I2 splice (IVS2 −12A/C>G) in combination with 707-714del (without the P30L mutation) was caused by multiple gene deletions (~30-kb deletion). Therefore, these polymorphic sites of nts 620, 624, 629–630, S108 (TCC>TCG), and S113 (TCC>TCT) (Table 2) in IVS2 were not presented in the 226-bp amplicon (Table 1) amplified with the paired primers, C100/In3R, and did not influence the HRM analysis (Table 2). In addition, the HRM profile (Fig. 2D) of the cluster E6 mutation in 2 (D1, I236N and V237E, sample #249) and 3 (D2, I236N, V237E, and M239K, sample #393) mutated sites showed two different melting plots. This indicated that the sequence with the heterozygous variant might show either an upcurved (sample #393) or a downcurved (sample #249) plots in this case. We are not sure that whether the polymorphic site of D234 (GAT>GAC), which is always bounded (Supplemental Fig. 1, D1, D2), can be attributed to the production of 2 different melting types. The polymorphic sites of nts 1420 (A>G) and 1421(C>T) not being included (data of DNA sequencing not shown) indicates that the occurrence of the intergenic conversion did not extend to these 2 polymorphic sites in these 2 mutation types.

In addition, the influence of different template concentrations in the HRM analysis should be considered in our study. In order to separate the *CYP21A2* gene from the *CYP21A1P* pseudogene, a primary 3.5-kb primary PCR product of the *CYP21A2* gene should be amplified first, and then the primary PCR product can be used as a template for the secondary PCR amplification by the HRM analysis. A nested PCR was carried out to identify mutations of the CYP21A2 gene, and the concentration of the primary PCR product was difficult to calculate. It was reported that a deviating curve can occasionally occur due to input of a higher amount of DNA (2.5×) that might give rise to a false-positive result [42].

In conclusion, a rapid, sensitive, and reliable strategy for mutation scanning of the *CYP21A2* gene using an HRM analysis was documented. As indicated above, we established a standard profile for the most common 11 mutation sites of the *CYP21A2* gene. This protocol can be used as a tool for screening most patients with CAH caused by defects of the *CYP21A2* gene converted from the CYP21A1P pseudogene.

Please cite this article as: Lin Y-C, et al, High-resolution melting curve (HRM) analysis to establish CYP21A2 mutations converted from the CYP21A1P in congenital adrenal hyperplasia, Clin Chim Acta (2011), doi:10.1016/j.cca.2011.06.033

Table 2
Polymorphic sites influencing the heteroduplex form in a specific fragment of the *CYP21A2* gene using the HRM analysis.

Mutational locus	Fragment (paired primer amplification)	Polymorphic site (exon/nucleotide)[a]		Interchange
		CYP21A2	*CYP21A1P*	
P30L	1A2/1AR	L39 (TTG)	(CTG)	?
		P45 (CCA)	(CCC)	?
I2 splice[b]	C100/In3R	nt 620 (A)	(G)	No
		nt 624 (G)	(T)	No
		nt 629/630 (C/A)	(G/G)	No
707–714 del	C100/In3R	S108 (TCC)	(TCG)	Yes
		S113 (TCC)	(TCT)	Yes
I172N	In3-1/E4r	–	–	–
Cluster E6 [c]	Ex6/C8	D234 (GAT)	(GAC)	Yes
		nt 1420/21 (A/C)	(G/T)	No
V281L,	C9/S7r	–	–	–
F306ΔL307insT	C9/S7r	–	–	–
Q318X	In7-1/C12-1	–	–	
R356W	In7-1/C12-1	–	–	–

[a] Based on Higashi et al. [6].
[b] I2 splice, IVS2 −12A/C>G, or nt 655.
[c] Cluster E6 represents I236N, V237E, and M239K.

Supplementary materials related to this article can be found online at doi:10.1016/j.cca.2011.06.033.

Acknowledgements

This study was supported by a grant from Kaohsiung Medical University Hospital (KMUH98-8G68).

References

[1] White PC, Speiser PW. Congenital adrenal hyperplasia due to 21-hydroxylase deficiency. Endocr Rev 2000;21:245–91.
[2] New MI, Wilson RC. Steroid disorders in children: congenital adrenal hyperplasia and apparent mineral corticoid excess. Pro Natl Acad Sci U S A 1999;96:12790–7.
[3] New MI. Extensive clinical experience nonclassical 21-hydroxylase deficiency. J Clin Endocrinol Metab 2006;91:4205–14.
[4] Therrel BL. Newborn screening for congenital adrenal hyperplasia. Endocrinol Metab Clin North Am 2001;30:15–30.
[5] Fitness J, Dixit N, Webster D, et al. Genotyping of CYP21, linked chromospme 6p marker, and a sex-specific gene in neonatal screening for congenital adrenal hyperplasia. J Clin Endocrinol Metab 1999;84:960–6.
[6] Higashi Y, Yoshioka H, Yamane M, Gotoh O, Fujii-Kuriyama Y. Complete nucleotide sequence of two steroid 21-hydroxylase genes tandemly arranged in human chromosome: a pseudogene and genuine gene. Proc Natl Acad Sci U S A 1986;83:2841–5.
[7] White PC, New MI, Doupont B. Structure of human steroid 21-hydroxylase genes. Proc Natl Acad Sci U S A 1986;83:5111–55.
[8] YusiÉ-Luna MT, White PC. Gene conversion and unequal crossovers between CYP21 (steroid 21-hydroxylase gene) and CYP21P involve different mechanisms. Proc Natl Acad Sci U S A 1995;92:10796–800.
[9] Chang SF, Lee HH. Analysis of the CYP21A2 gene with intergenic recombination and multiple gene deletions in the RCCX module. Genet Test Mol Biomarkers 2011;15:35–42.
[10] Koppens PFJ, Hoogenboezem T, Degenhart HJ. Carriership of a defective tenascin-X gene in steroid 21-hydroxylase deficiency patients: TNXB–TNXA hybrids in apparent large-scale gene conversions. Hum Mol Genet 2002;11:2581–90.
[11] Lee HH. Chimeric CYP21P/CYP21 and TNXA/TNXB genes in the RCCX module. Mol Genet Metab 2005;84:4–8.
[12] Vrzalová Z, Hrubá Z, Hrabincová ES, et al. Chimeric CYP21A1P/CYP21A2 genes identified in Czech patients with congenital adrenal hyperplasia. Eur J Med Genet 2011;54:112–7.
[13] Tsai LP, Cheng CF, Chuang SH, Lee HH. Analysis of the CYP21A1P pseudogene: indication of mutational diversity and CYP21A2-like and duplicated CYP21A2 genes. Anal Biochem 2011;413:133–41.
[14] Lee HH, Lee YJ, Wang YM, et al. Low frequency of the CYP21A2 deletion in ethnic Chinese (Taiwanese) patients with 21-hydroxylase deficiency. Mol Genet Metab 2008;93:450–7.
[15] Dain LB, Buzzalino ND, Oneto A, et al. Classical and nonclassical 21-hydroxylase deficiency: a molecular study of Argentine patients. Clin Endocrinol 2002;56:239–45.
[16] Stikkelbroeck NMML, Hoefsloot LH, de Wijs IJ, Otten BJ, Hermus ARMM, Sistermans EA. CYP21 Gene mutation analysis in 198 patients with 21-hydroxylase deficiency in the Netherlands: six novel mutations and a specific cluster of four mutations. J Clin Endocrinol Metab 2003;88:3852–9.
[17] Friaes A, Rego AT, Aragues JM, et al. CYP21A2 mutations in Portuguese patients with congenital adrenal hyperplasia: identification of two novel mutations and characterization of four different partial gene conversions. Mol Genet Metab 2006;88:58–65.
[18] Tsai LP, Cheng CF, Hsieh JP, Teng MS, Lee HH. Application of the DHPLC method for mutational detection of the CYP21A2 gene in congenital adrenal hyperplasia. Clin Chim Acta 2009;410(1–2):48–53.
[19] Koyama S, Toyoura T, Saisho S, Shmozawa K, Yata J. Genetic analysis of Japanese patients with steroid 21-hydroxylase deficiency: identification of a patient with a new mutation of a homozygous deletion of adenine at codon 246 and patients without demonstrable mutations within the structural gene for CYP21. J Clin Endocrinol Metab 2002;87:2668–73.
[20] Kharrat M, Tardy V, M'rad R, et al. Molecular genetic analysis of Tunisian patients with a classic form of 21-hydroxylase deficiency: identification of four novel mutations and high prevalence of Q318X mutation. J Clin Endocrinol Metab 2004;89:368–74.
[21] Lee HH. CYP21 mutations and congenital adrenal hyperplasia. Clin Genet 2001;59:293–301.
[22] Keen-Kim D, Redman JB, Alanes RU, Eachus MM, Wilson RC, New MI, et al. Validation and clinical application of a locus-specific polymerase chain reaction- and minisequencing based assay for congenital adrenal hyperplasia (21-hydroxylase deficiency). J Mol Diagn 2005;7:236–46.
[23] Owerbach D, Crawford YM, Draznin MB. Direct analysis of CYP21B genes in 21-hydroxylase deficiency using polymerase chain reaction amplification. Mol Endocrinol 1990;4:125–31.
[24] Day DJ, Speiser PW, White PC, Barany F. Detection of steroid 21-hydroxylase alleles using gene-specific PCR and a multiplexed ligation detection reaction. Genomics 1995;29:152–62.
[25] Loidi L, Quinteiro C, Parajes S, et al. High variability in CYP21A2 mutated alleles in Spanish 21-hydroxylase deficiency patients, six novel mutations and a founder effect. Clin Endocrinol 2006;64:330–6.
[26] Tajima T, Fujieda K, Nakayama K, Fujii-Kuriyama Y. Molecular analysis of patients and carrier genes with congenital steroid 21-hydroxylase deficiency by using polymerase chain reaction and single strand conformational polymorphism. J Clin Invest 1993;92:2182–90.
[27] Lee HH, Chao HT, Ng HT, Choo KB. Direct molecular diagnosis of CYP21 mutations in congenital adrenal hyperplasia. J Med Genet 1996;33:371–5.
[28] Olney RC, Mougey EB, Wang J, Shulman DI, Sylvester JE. Using real-time, quantitative PCR for rapid genotyping of the steroid 21-hydroxylase gene in a north Florida population. J Clin Endocrinol Metab 2002;87:735–41.
[29] Krone N, Braun A, Weinert S, Peter M, Roscher AA, Partsch CJ, et al. Multiplex minisequencing of the 21-hydroxylase gene as a rapid strategy to confirm congenital adrenal hyperplasia. Clin Chem 2002;48:818–25.
[30] Zeng X, Witchel SF, Dobrowolski SF, Moulder PV, Jarvik JW, Telmer CA. Detection and assignment of CYP21 mutations using peptide mass signature genotyping. Mol Genet Metab 2004;82:38–47.
[31] Concolino P, Mello E, Toscano V, Ameglio F, Zuppi C, Capoluongo E. Multiple ligation-dependent amplification (MLPA) assay for the detection of CYP21A2 gene deletions/duplications in congenital adrenal hyperplasia: first technical report. Clinca Chimica Acta 2009;402:164–70.
[32] Lee HH, Chao MC, Lee YJ. Only two amino acid substitutions of I236N and V237E in exon 6 are converted to the CYP21 gene in a Chinese patient with congenital adrenal hyperplasia. Clin Endocrinol 2006;64:227–9.
[33] Robins T, Barbaro M, Lajic S, Wedell A. Not all amino acid substitutions of the common cluster E6 mutation in CYP21 cause congenital adrenal hyperplasia. J Clin Endocrinol Metab 2005;90:2148–53.
[34] New MI. An update of congenital adrenal hyperplasia. Ann N Y Acad Sci 2004;1038:14–43.
[35] Jones AC, Sampson JR, Cheadle JP. Low level mosaicism detectable by DHPLC but not by direct sequencing. Hum Mutat 2001;17:233–4.
[36] Dobrowolski S, Gray J, Miller T, Sears M. Identifying sequence variants in the human mitochondrial genome using high-resolution melt (HRM) profiling. Hum Mutat 2009;30:891–8.
[37] Vossen RHAM, Aten E, Roos A, den Dunnen JT. High-resolution melting analysis (HRMA)—more than just sequence variant screening. Hum Mutat 2009;30:860–6.
[38] Leiden Genome Technology Center (LGTC) Published assays using high-resolution melting analysis (HRMA).. http://www.LGTC.nl/HRMA.
[39] Reed GH, Wittwer CT. Sensitivity and specificity of single-nucleotide polymorphism scanning by high-resolution melting analysis. Clin Chem 2004;50:1748–54.
[40] Takano EA, Mitchell G, Fox1 SB, Dobrovic A. Rapid detection of carriers with *BRCA1* and *BRCA2* mutations using high resolution melting analysis. BMC Cancer 2008;8:59.
[41] Shih HC, Er TK, Chang TJ, Chang YS, Liu TC, Chang JG. Rapid identification of HBB gene mutations by high-resolution melting analysis. Clin Biochem 2009;42:1667–76.
[42] van der Stoep N, van Paridon CD, Janssens T, Krenkova P, Stambergova A, Macek M, et al. Diagnostic guidelines for high-resolution melting curve (HRM) analysis: an interlaboratory validation of BRCA1 mutation scanning using the 96-well LightScanner. Hum Mutat 2009;30:899–909.

Please cite this article as: Lin Y-C, et al, High-resolution melting curve (HRM) analysis to establish CYP21A2 mutations converted from the CYP21A1P in congenital adrenal hyperplasia, Clin Chim Acta (2011), doi:10.1016/j.cca.2011.06.033